



Published in final edited form as:

Kidney Int. 2014 January ; 85(1): 124–133. doi:10.1038/ki.2013.354.

Exome sequencing and in vitro studies identified podocalyxin as a candidate gene for focal and segmental glomerulosclerosis

Moumita Barua^{1,2,+}, Eric Shieh^{2,+}, Johannes Schlondorff^{1,2}, Giulio Genovese^{3,4,5}, Bernard S Kaplan⁶, and Martin R Pollak^{1,2}

¹Division of Nephrology, Dept. of Medicine, Beth Israel Deaconess Medical Center, Boston, MA

²Harvard Medical School, Boston, MA

³Stanley Center for Psychiatric Research, Cambridge, MA

⁴Program in Medical and Population Genetics, Broad Institute of MIT and Harvard, Cambridge, MA

⁵Department of Genetics, Harvard Medical School, Boston, MA

⁶Department of Pediatrics, Division of Nephrology, The Children's Hospital of Philadelphia, Philadelphia, PA

Abstract

Our understanding of focal and segmental glomerulosclerosis (FSGS) has advanced significantly from the studies of rare, monogenic forms of the disease. These studies have demonstrated the critical roles of multiple aspects of podocyte function in maintaining glomerular function. A substantial body of research has suggested that the integral membrane protein podocalyxin (PODXL) is required for proper function of podocytes, possibly by preserving the patency of the slit diaphragm by negative charge-based repulsion. Exome sequencing of affected cousins from an autosomal dominant pedigree with FSGS identified a co-segregating private variant, *PODXL* p.L442R, affecting the transmembrane region of the protein. Of the remaining 11 shared gene variants, two segregated with disease but their gene products were not detected in the glomerulus. In comparison to wild type, this disease-segregating *PODXL* variant facilitated dimerization. By contrast, this change does not alter protein stability, extracellular domain glycosylation, cell surface expression, global subcellular localization, or interaction with its intracellular binding partner ezrin. Thus, a variant form of *PODXL* remains the most likely candidate causing FSGS in one family with autosomal dominant inheritance, but its full effect on protein function remains unknown. Our work highlights the challenge faced in the clinical interpretation of whole exome data for small pedigrees with autosomal dominant diseases.

Users may view, print, copy, and download text and data-mine the content in such documents, for the purposes of academic research, subject always to the full Conditions of use:http://www.nature.com/authors/editorial_policies/license.html#terms

Correspondence: Martin Pollak, 99 Brookline Avenue, Rm 304, Boston, MA, 02215, Office: 617-667-0496, Fax: 617-667-0495, mpollak@bidmc.harvard.edu.

⁺Contributed equally to this work

DISCLOSURES

None

Introduction

Focal and segmental glomerulosclerosis (FSGS) is a histologically defined form of kidney injury characterized by the presence of sclerosis in parts of some but not all glomerular tufts. Patients with FSGS are challenging to treat due to their frequently relapsing course and a high rate of progression to end-stage kidney disease (ESRD).^{1, 2} FSGS is also the most common glomerular lesion underlying ESRD in the United States, thus representing a significant burden to health care.^{3, 4}

Over the past two decades, our understanding of FSGS pathogenesis has advanced significantly. Some of these advances have come from the study of rare, monogenic forms. These studies have been instrumental in identifying the slit diaphragm and actin cytoskeleton of podocytes as critical elements in maintaining glomerular function. This notion has been supported by the fact that podocyte injury and dysfunction is an almost universal aspect of proteinuric glomerular diseases.⁵

A substantial body of research has suggested that a negatively-charged, heavily glycosylated integral membrane protein, podocalyxin (PODXL), is required for the proper function of podocytes as glomerular filters.^{6, 7} PODXL is thought to act as an anti-adhesin that maintains the patency of the filtration slits between adjacent podocytes through charge repulsion.^{8, 9} Neutralization of podocytes' negative charge in rats results in podocyte injury, nephrosis, and massive proteinuria, and in humans, PODXL expression is reduced in several proteinuric glomerulopathies.^{6, 10-16} Mice deficient in PODXL demonstrate defective podocyte foot-process formation, with resulting anuria and renal failure leading to death within 24 hours of birth. Taken together, these data suggest that abnormal PODXL activity represents a common mechanism in some kidney diseases and that PODXL function is required for normal podocyte function.

The present study began with the analysis of the exome sequence of two individuals from a family with childhood onset FSGS. This analysis revealed a previously unreported non-synonymous *PODXL* variant in these two individuals. Subsequently, we sequenced the entire *PODXL* gene in 176 probands with a familial inheritance pattern consistent with autosomal dominant FSGS. We identified five rare non-synonymous variants, though three of these additional variants were also found in publicly available exome databases of nominally normal persons. In addition, we observe that numerous additional rare non-synonymous variants in *PODXL* are also present in these public databases. We performed several biochemical and cell biological analyses to examine the effects of several of these variants, with only the index case mutation demonstrating an effect on the biochemical properties of the protein. Taken together, this study suggests a causal role for variation in *PODXL* in the etiology of very rare cases of FSGS, but illustrates the difficulty in definitively identifying rare mutations as disease causing.

Results

Exome sequencing was performed on genomic DNA samples belonging to two cousins, III(3) and III(4) (Figure 1a). After filtering, non-synonymous missense variants were

identified in 12 different genes that were present in both individuals studied (Supplementary table 1). Coverage of these loci was highly variable, ranging from 3× to 68× per individual. Even at low coverage, variants were included in the list of candidate genes selected for followup analysis if seen in both individuals, as the likelihood of this occurring by chance alone is small. All of the variants of interest were also confirmed by Sanger sequencing and sequenced in the additional related family members. DNA samples were available for affected individuals II(2), II(8), III(3), III(4) and III(5); as well as for unaffected individuals II(7) and III(2). The variants in the genes *C6orf103*, *OR9A2* and *PODXL* cosegregated with disease.

C6orf103 is expressed fairly widely, with most normal tissues displaying moderate to strong cytoplasmic staining. In the human kidney, however, *C6orf103* stains strongly in tubules but not in glomeruli (<http://www.proteinatlas.org/ENSG00000118492/normal>). Its function is unknown. Similarly, in the human kidney, *OR9A2* stains in the tubules but is absent in glomeruli (Supplementary figure 1). This gene is also in proximity to *PODXL*, approximately 11 megabases apart. *OR9A2* is an olfactory receptor that interacts with odorant molecules in the nose. No additional novel variants in these 2 genes, *C6orf103* and *OR9A2*, were identified in screening 80 probands from families with FSGS. Conversely, *PODXL* stains distinctly in glomerular podocytes and in few additional cell types (<http://www.proteinatlas.org/ENSG00000128567/normal>). A substantial body of research has shown an integral role of *PODXL* to glomerular function. As a result, the variant in *PODXL* was selected for further study given this gene's known role in glomerular biology.

Coverage by next-generation sequencing at the *PODXL* variant was 9× and 18×, for individuals III(3) and III(4), respectively and confirmed by Sanger sequencing (Figure 1b, 1c). The *PODXL* variant is predicted to change a highly conserved residue in most vertebrates, a non-polar leucine into a charged arginine (p.L442R), within the transmembrane domain of the *PODXL* protein (Figure 1d).

The clinical information for family FG-HI has been previously reported.¹⁷ The affected index case in the pedigree I(1) (b. 1931), was diagnosed with renal disease in his early 20s. He developed ESRD at age 28 and died without receiving renal replacement therapy. He had 4 children, 3 of whom carry the *PODXL* variant but only 2 with clinically detectable renal disease. DNA belonging to the fourth child who is unaffected, II(4), was not available for testing. Individual II(2) (b. 1955) was identified to have proteinuria and an elevated creatinine at age 26 during a routine pre-employment examination. A renal biopsy showed FSGS and he was treated conservatively without immunomodulatory therapy. At the age of 55, he received a living related kidney transplant. Another child, II(8) (b. 1959), was also detected to have proteinuria but not an elevated creatinine during a pre-employment examination at the age of 19. Within 4 years, he developed ESRD, initially treated with intermittent hemodialysis before receiving a living related kidney transplant. The graft failed after 15 years for unclear reasons but he eventually received a deceased donor kidney in 1988. In 2011, his creatinine was 2.1 mg/dL with no proteinuria.

Four grandchildren of I(1), belonging to the youngest generation of this pedigree are affected, three of whom had DNA available and harbor the *PODXL* variant. The most

severely affected is III(4) (b. 1990) presenting with lower extremity edema at age 12 and subsequently found to have 4+ proteinuria along with an elevated creatinine. She received peritoneal dialysis for less than a year before receiving a living related kidney transplant at the age of 14 with good graft function. Her older sister, III(5) (b. 1989), was screened as a result and found to have 4+ proteinuria. She did not have a renal biopsy and has been managed conservatively without evidence of chronic kidney disease. A cousin, III(3) (b. 1989), was screened for disease because of this family history and found to have proteinuria at the age of 13. She did not have a kidney biopsy and has been managed conservatively. Her sister, III(2) (b. 1991) is also monitored closely with no evidence of renal dysfunction. Finally, another cousin, III(6) (b. 1995) is also affected. He was found to have 3+ proteinuria several years ago but has not been monitored since then. DNA from this individual was not available for testing.

To ascertain whether mutations in *PODXL* were present in other autosomal dominant FSGS families, we sequenced *PODXL* in DNA from 176 probands with presumed autosomal dominant FSGS. We identified 4 additional individuals with rare variants in *PODXL* coding sequence. However, analysis of available exome sequencing data from both the 1000 Genomes Project and the Exome Sequencing Project revealed that three of these variants have been found in nominally normal individuals, leaving a single additional private variant not found previously. This variant, p.S214R, was detected in family FG-IX, which harbors another private mutation in a second gene that has also been linked to kidney disease (MB, GG, MRP; unpublished data). DNA was not available from any of the other affected individuals. The frequency of rare non-synonymous variants in the *PODXL* gene was not different between cases and controls in the Exome Sequencing Project (ESP), indicating that the burden of rare variants was not enriched in cases. Taken together, these data suggest that rare variation in *PODXL* are not a significant contributor to glomerular disease.

In light of suggestive but not definitive genetic evidence that any of these *PODXL* variants we identified contributed to disease, we examined whether any of these variants affected protein behavior, as has been demonstrated for disease-causing mutations in *ACTN4*, *TRPC6* and *INF2*.^{18–22} We were particularly interested in whether the private *PODXL* variants p.L442R and p.S214R behaved differently from the three non-unique variants identified in our FSGS cohort and the four variants found in ESP (Table 1). Western blot analysis of transiently transfected MDCK cells did not reveal any apparent differences in the quantity of protein expressed between the suspected *PODXL* disease-causing mutations and “control” variants or wildtype protein (Figure 2).

While the quantity of the protein expressed was not affected, the *PODXL* construct containing the p.L442R variant produced a higher molecular weight form in addition to a normally sized product. By SDS-PAGE, *PODXL* p.L442R expressed in MDCK cells and lysed in mild lysis buffer (TBS + 1% NP-40) was detected as two bands: a ~330 kDa upper band and a ~165 kDa lower band (Figure 2, lane 2). By contrast, the other variants and the wildtype protein were detected primarily as ~165 kDa bands under the same experimental conditions. We suspect that the upper band observed for the *PODXL* p.L442R mutant may represent a dimer of the protein given its molecular weight, though we cannot exclude the alternative possibility that it represents aggregation with an unrelated protein.⁷

To determine if differential extracellular domain glycosylation accounted for the higher molecular form, we treated cell lysates with either PNGase F to remove N-glycosylations; neuraminidase to remove sialic acid motifs; or a combination of O-glycosidase and neuraminidase to remove O-glycosylations. No significant differences were seen between the glycosylation patterns of wildtype and PODXL p.L442R mutant on Western blotting, indicating that the mutation has little effect on the glycosylation of the protein (Figure 3a). We then investigated the effect of different lysis buffers on the abundance of the two forms of PODXL p.L442R. Lysing cells in RIPA buffer prevented the formation of the dimer, suggesting that the upper band is an aggregate generated during cell lysis with non-ionic detergent (Figure 3b).

PODXL is predominately localized to the apical surface of podocytes and MDCK cells and some protein is associated with endoplasmic reticulum, Golgi complexes, and cytoplasmic vesicles.^{23, 24} To investigate whether the L442R mutation alters the subcellular localization and surface expression of PODXL, we performed confocal immunofluorescence microscopy and cell surface biotinylation experiments. Confocal immunofluorescence microscopy showed similar staining patterns for wildtype and PODXL p.L442R mutant, with punctate staining along the apical surface of the cell (Figure 4a, b). Biotinylation experiments served to quantitatively examine cell surface expression; the fraction of PODXL protein reaching the cell surface did not appear to be different between wildtype or mutant on Western blot (Figure 4c).

PODXL has been reported to complex ezrin to link to the actin cytoskeleton.^{25, 26} Mutations in other FSGS genes such as *ACTN4* and *INF2* have been shown to disrupt the actin cytoskeleton thus this represents a plausible common mechanism of injury.^{27, 28} The ability of wildtype and PODXL p. L442R to colocalize with ezrin was compared; both forms demonstrated partial colocalization with overexpressed ezrin (Figure 5).

Discussion

Exome sequencing of two affected individuals belonging to a family with autosomal dominant FSGS revealed a novel variant in a highly attractive candidate gene, *PODXL*. This gene encodes a transmembrane sialoglycoprotein localized to the podocyte apical surface and is presumed to keep adjacent foot processes separated by virtue of its negative charge, thereby serving an essential role in glomerular filtration as supported by knockout studies in mice. Further screening in 176 probands revealed an additional private mutation in only one other individual where no other affected samples were available, leading to a lack of strong statistical genetic evidence to support *PODXL* as a disease gene. In view of this, several biochemical and cell biological analyses were undertaken involving the two identified private variants as well as additional rare variants found in cases and controls. Only the index case mutation located in the transmembrane domain, PODXL p.L442R, demonstrated a differential effect, with our results suggesting that the mutant form promotes dimerization. Further experiments showed that the mutation, however, does not alter: 1. protein stability 2. extracellular domain glycosylation 3. cell surface expression 4. global subcellular localization, or 5. interaction with its intracellular binding partner ezrin.

Twelve shared rare variants were identified between two affected cousins in the pedigree FG-HI. The variant in *PODXL* cosegregated with disease, though with incomplete penetrance in this family. Screening 176 additional probands revealed only a single other private mutation but in a family where no other samples were available. Furthermore, the burden of rare non-synonymous variants was not enriched in the cases versus controls and therefore collectively the statistical support for this gene was not strong. Sequencing for cosegregation for the remaining 11 shared variants was also performed, leaving only 2 additional novel candidates: *C6orf103* and *OR9A2*. *C6orf103* is expressed fairly widely but only in tubular and not glomerular cells in the kidney. Its function is unknown. Similarly, *OR9A2* is expressed in the tubules but not glomerular cells. The gene coding this protein is also in close proximity to *PODXL*. *OR9A2* is known to be an olfactory receptor that interacts with odorant molecules in the nose. Neither of these has compelling biological data to indicate an obvious link to FSGS. We were also unable to identify novel variants in the two genes, *C6orf103* and *OR9A2*, in screening 80 additional FSGS families.

Similar to other monogenic forms of later onset FSGS, disease severity in this family is variable. Disease onset occurs in the teenage to early adulthood years but ESRD occurs widely from the second to sixth decade of life. Interestingly, disease penetrance in this family is incomplete. All three generations are affected, consistent with autosomal dominant inheritance but individual II(7), who is an obligate carrier, does not have clinically detectable renal disease, with her last examination occurring at age 53 years. The explanation for why this individual did not manifest disease is unclear but since it is reasonable to assume that she and her affected daughters and brothers were exposed to similar environments, a gene-gene interaction may provide a plausible explanation.

With biochemical and cell-based experiments, we provide evidence that the transmembrane variant *PODXL* p.L442R facilitates dimerization of the protein. We have not, however, been able to establish the effect of this biochemical change on the function of *PODXL*, nor can we exclude that this property is solely unmasked after cell lysis. We have shown that the mutation does not alter protein stability, extracellular domain glycosylation, cell surface expression, global subcellular localization, or interaction with its intracellular binding partner ezrin. Our working hypothesis that the variant might lead to (a) reduced negative charge at the apical membrane resulting in disruption of filtration slit patency or (b) alteration in actin cytoskeleton dynamics through interference with ezrin, an actin binding protein, is not supported by our experimental data.^{25, 26, 29–31}

Given these observations, it is still conceivable then that altered multimerization of *PODXL* alone could affect proper assembly/disassembly into the larger multiprotein complex it forms with other proteins including *CLIC5A* and *NHERF*. Previous reports have shown that *PODXL* can form dimers, which likely represent a more mature form of the protein.^{7, 32} One group has suggested a model in which nascent *PODXL* is initially monomeric and is subsequently clustered into dimers through the binding of *PODXL* to the intracellular adaptor protein *NHERF2*.³³ Our result of the *PODXL* p.L442R variant enhancing dimerization suggests that the transmembrane domain of the protein may play a key role in regulating the high-order aggregation of the protein with itself and other binding partners.³³

More detailed cell biological and biochemical analysis, including those involving ezrin and other binding partners, are needed to explore this possibility.

We point out that exome capture coupled with next-generation sequencing is associated with a higher false positive rate than Sanger sequencing. By sequencing the exome of 2 affected individuals, we reduce the error introduced by false positive variants as the possibility of observing falsely occurring variants in two samples is statistically very low. However, an inherent limitation with subgenomic capture is the heterogenous enrichment of the target and lack of variant calls in certain regions. As a result, we may have excluded some candidate genes. We also point out that we used MDCK cells for these studies rather than a native human kidney cell line. Other groups have also used MDCK cells as a surrogate to examine PODXL characteristics given the cells' columnar morphology, which allows for the study of apical and basolateral localization.³⁴⁻³⁶ Despite several attempts, we were unable to obtain efficient expression of PODXL in cultured podocytes for study.

The conclusions we draw from this study are two-fold. *PODXL* is a candidate causative gene in a single family under study, based on suggestive but not definitive genetic data and abnormal dimerization of the mutant protein. Secondly, the lack of *in vitro* evidence beyond apparent dimerization supporting *PODXL* p.L442R mutant pathogenicity highlights the insensitivity of *in vitro* techniques to help support or refute a candidate gene as disease causing. We note that these issues will be increasingly common in the era of exome and whole genome sequencing, which offers the potential of uncovering culprit genes in small, previously uninformative autosomal dominant families but at the expense of generating cumbersome lists of candidate genes. This is in contrast to early onset autosomal recessive conditions, especially in pedigrees with consanguinity, where exome sequencing has been highly successful by narrowing the list of suspicious variants to those that affect both alleles of a single gene. The difficulties in reaching definitive conclusions even in a research setting with the added benefit of multiple affected family members and the willingness to pursue follow up biochemical studies suggests that clinical application of these methods to autosomal dominant disease will be fraught with difficulties.

Concise Methods

Patients

Individuals belonging to 176 families with FSGS were included in this study. Familial cases were defined as 2 or more affected individuals. All families had an inheritance pattern consistent with autosomal dominance. Familial FSGS affected status was defined as having either a reported history of proteinuria, nephrotic syndrome or biopsy-proven FSGS, having documented proteinuria with urine microalbumin >250mg/g creatinine in a family with at least one other case of documented FSGS or nephrotic syndrome. Most of these families had previously been screened for mutations in known genes including *INF2*, *TRPC6* and *ACTN4*. We obtained blood, saliva, or isolated DNA and clinical information after receiving informed consent from participants in accordance with the Institutional Review Board at the Beth Israel Deaconess Medical Center. Clinical information was obtained from telephone interviews, questionnaires and physician reports. Genomic DNA was extracted from blood or saliva samples using standard procedures.

Exome and next-generation sequencing

We performed exome sequencing in two affected individuals of a family with FSGS. A shotgun library was made from each individual's genomic DNA and captured using the NimbleGen SeqCap EZ Exome v2 (NimbleGen, Madison, WI) according to protocol. The manufacturer's specifications state that the capture regions total approximately 44 Mb. This kit covers 98% of the human genome corresponding to the Consensus Conserved Domain Sequences database (CCDS) and 710 miRNAs. Enriched libraries were then sequenced by 46 base pair, paired end read sequencing on an Illumina GAI machine according to protocol (Illumina Inc, San Diego, CA). Variants of interest were confirmed by Sanger sequencing.

Variant analysis

Next-generation sequencing reads were mapped to the most recent reference human genome (UCSC hg19), with bwa.³⁷ The Genome Analysis Toolkit was used to further process the aligned read data, and the same program was used to genotype the individuals from the processed read data.^{38, 39} Variants were filtered by comparison to the other related affected individual sent for exome sequencing—variants that appeared in both affected individuals remained in the analysis, even at low coverage given the unlikely possibility of this happening by chance. If a variant was seen at low coverage in one sample but not in the other due to non-capture, it was kept in the analysis as well. For all sequencing data produced, whether by Sanger method or next-generation sequencing, genotype calls were compared against dbSNP 134 (<ftp://ftp.ncbi.nih.gov/snp/>), 1000 Genomes Project (<ftp://ftp.1000genomes.ebi.ac.uk/vol1/ftp/>) and the Exome Sequencing Project (<http://evs.gs.washington.edu/EVS/>).

Sanger Sequencing

Sanger sequencing was performed on the remaining FSGS samples using Big Dye 3.1 terminator cycle sequencing kit (Life Technologies, Grand Island, NY) and analyzed with an ABI Prism 3730 XL DNA analyzer (Applied Biosystems, Foster City, California). Primer sequences are available on request. Sequence chromatograms were analyzed using the Sequencher software (Gene Codes, Ann Arbor, MI). Specific variants identified in family probands were sequenced in all available family members to investigate if the variant segregated with disease (Supplementary Figure 1). If an affected individual did not harbor the variant of interest, it was excluded as disease causing.

Reagents and plasmids

A plasmid containing the full-length human PODXL cDNA (transcript variant 2) was obtained from Origene and was mutated to remove the carboxyl-terminal epitope tags. The indicated coding mutants were introduced by site-directed mutagenesis (QuickChange II XL, Stratagene). All plasmids were sequenced to confirm the presence of mutations and exclude the presence of unwanted mutations. GFP-tagged ezrin in pEGFP-N2 was provided by A. Bretscher (Weill Institute for Cell and Molecular Biology, Cornell University, Ithaca, NY; PMID 22801783). Antibodies were obtained from commercial sources as follows: anti-PODXL 3D3 mouse monoclonal (Santa Cruz), anti-GFP full-length rabbit polyclonal (Santa Cruz) and HRP conjugated secondary antibodies (Cell Signaling Technologies).

Cell culture

Madin-Darby canine kidney (MDCK) Tet-Off cells were obtained from Clontech and maintained as per the manufacturer's recommendations. Transient transfections were performed using Lipofectamine 2000 (Invitrogen) following the manufacturer's protocol. 16 to 24 hours after transfection, cells were washed once in PBS and then lysed in 300 μ l of ice-cold RIPA lysis buffer (50 mM Tris pH 7.4, 150 mM NaCl, 1% NP-40, 1% sodium deoxycholate, 0.1% SDS) or TBS with 1% (v/v) Nonidet P-40 lysis buffer supplemented with Complete Protease Inhibitor Cocktail and PhosSTOP Phosphatase Inhibitor Cocktail (Roche).

Western blot analysis

Cell lysates were cleared by centrifugation at 14,000 g for 15 minutes at 4°C. The resulting supernatant was mixed with sample loading buffer, separated by SDS-PAGE, and transferred to polyvinylidene difluoride membrane (Bio-Rad). Western blot analysis was performed using standard techniques with primary antibodies used at the following dilutions: anti-PODXL (1:1000), anti-GFP (1:1000). Blots were developed with SuperSignal West Dura Chemiluminescent Substrate (Pierce) and a Fluorochem Q imager (Cell Biosciences).

Immunofluorescence confocal microscopy

MDCK cells were plated on collagen I-coated coverslips (BD) and transfected with lipofectamine 2000 (Invitrogen). After 16–24 hours, cells were fixed in 2% paraformaldehyde, 4% sucrose in PBS for 10 minutes at room temperature and permeabilized with 0.3% (v/v) Triton X-100 in PBS for 10 minutes. Nonspecific binding sites were blocked using blocking solution (2% (v/v) fetal bovine serum, 2% (w/v) bovine serum albumin, 0.2% fish gelatin in PBS) for 30 minutes at room temperature. For localization, cells were incubated with 1:50 anti-PODXL antibody for 1 hour, followed by incubation with 1:500 Dylight 594 goat anti-mouse antibodies (Thermo Scientific) for 1 hour. Cells were counterstained with AlexaFluor 488 Phalloidin and Hoechst 33342 (Invitrogen). For colocalization with ezrin experiments, cells were incubated with 1:50 anti-PODXL antibody as well as 1:50 anti-GFP antibody for 1 hour, followed by incubation with 1:500 Dylight 594 goat anti-mouse antibodies (ThermoScientific) and 1:50 AlexaFluor 488 goat anti-rabbit antibodies (Invitrogen) for 1 hour. Cells were mounted with Fluoromount-G (Southern Biotech). Confocal fluorescent images were obtained by a Zeiss LSM510NLO confocal scan head mounted on a Zeiss Axiovert 200M on an inverted-based microscope with a 63 \times objective and 0.1 μ m sections. Images were analyzed by Zeiss software.

Cell surface biotinylation

16 to 24 hours after transient transfection, cells were labeled with 0.5 mg/ml Sulfo-NHS-biotin (Thermo Scientific), followed by quenching in ice-cold TBS with 10mM glycine following the manufacturer's recommendations. Cells were subsequently lysed in TBS with 1% (v/v) Nonidet P-40, Complete Protease Inhibitor and PhosSTOP Phosphatase Inhibitor Cocktail (Roche). Lysates were briefly cleared by centrifugation. An aliquot of lysate was set aside and mixed with sample loading buffer. The remaining lysate was incubated with 20

ul of a 50% slurry of streptavidin beads (Pierce) at 4°C for 2 hours. After extensively washing the beads, bound material was eluted by boiling in sample loading buffer. Total and biotinylated PODXL were detected by Western blot analysis as above.

Deglycosylation

Cell lysates were either mock treated or treated with peptide *N*-glycosidase F, neuraminidase, or O-glycosidase and neuraminidase (PNGase F; O-Glycosidase & Neuraminidase Bundle; New England Biolabs) as per the manufacturer's recommendations, followed by SDS-PAGE and Western blot analysis.

Immunohistochemistry

Formalin-fixed human testis and kidney tissue was paraffin-processed and sectioned at 4 µm. After processing for antigen retrieval (pressure cooker in citrate buffer pH 6), sections were treated with antibodies against OR9A2 (1:200, rabbit polyclonal, LSBio) followed by Polymer-HRP secondary antibodies (Dako), and counterstained with hematoxylin. Images of representative glomeruli were taken with an Olympus BX53 microscope equipped with an Olympus DP72 camera.

Supplementary Material

Refer to Web version on PubMed Central for supplementary material.

Acknowledgments

M.B. is supported by a training fellowship from the Kidney Research Scientist Core Education and National Training Program, Canadian Society of Nephrology, and Canadian Institutes of Health Research. E.S. was supported by a summer scholarship from the American Society of Nephrology. This work was also supported by grants from the US National Institutes of Health (DK54931 to M.R.P.; DK080947 to J.S.; NHLBI/NHGRI Exome Project grant R01HL094963) and the NephCure Foundation (M.R.P).

We thank the families for their participation. The authors thank Andrea Uscinski Knob, MSc and Najwah Hayman for their assistance in obtaining clinical information, Drs. Christine and Jonathan Seidman for assistance with exome capture, Dr. Anthony Bretscher for providing the GFP-tagged ezrin in pEGFP-N2 construct and Sneha Krishna for technical assistance. The authors would also like to thank the NHLBI GO Exome Sequencing Project and its ongoing studies which produced and provided exome variant calls for comparison: the Lung GO Sequencing Project (HL-102923), the WHI Sequencing Project (HL-102924), the Broad GO Sequencing Project (HL-102925), the Seattle GO Sequencing Project (HL-102926) and the Heart GO Sequencing Project (HL-103010).

References

1. Rydel JJ, Korbet SM, Borok RZ, et al. Focal segmental glomerular sclerosis in adults: presentation, course, and response to treatment. *American journal of kidney diseases : the official journal of the National Kidney Foundation*. 1995; 25:534–542. [PubMed: 7702047]
2. Korbet SM, Schwartz MM, Lewis EJ. Primary focal segmental glomerulosclerosis: clinical course and response to therapy. *American journal of kidney diseases : the official journal of the National Kidney Foundation*. 1994; 23:773–783. [PubMed: 8203357]
3. D'Agati VD, Kaskel FJ, Falk RJ. Focal segmental glomerulosclerosis. *N Engl J Med*. 2011; 365:2398–2411. [PubMed: 22187987]
4. Kitiyakara C, Eggers P, Kopp JB. Twenty-one-year trend in ESRD due to focal segmental glomerulosclerosis in the United States. *American journal of kidney diseases : the official journal of the National Kidney Foundation*. 2004; 44:815–825. [PubMed: 15492947]

5. Somlo S, Mundel P. Getting a foothold in nephrotic syndrome. *Nat Genet.* 2000; 24:333–335. [PubMed: 10742089]
6. Kerjaschki D, Sharkey DJ, Farquhar MG. Identification and characterization of podocalyxin--the major sialoprotein of the renal glomerular epithelial cell. *The Journal of cell biology.* 1984; 98:1591–1596. [PubMed: 6371025]
7. Dekan G, Gabel C, Farquhar MG. Sulfate contributes to the negative charge of podocalyxin, the major sialoglycoprotein of the glomerular filtration slits. *Proc Natl Acad Sci U S A.* 1991; 88:5398–5402. [PubMed: 2052617]
8. Schnabel E, Dekan G, Miettinen A, et al. Biogenesis of podocalyxin--the major glomerular sialoglycoprotein--in the newborn rat kidney. *Eur J Cell Biol.* 1989; 48:313–326. [PubMed: 2744005]
9. Nielsen JS, McNagny KM. The role of podocalyxin in health and disease. *Journal of the American Society of Nephrology : JASN.* 2009; 20:1669–1676. [PubMed: 19578008]
10. Seiler MW, Rennke HG, Venkatachalam MA, et al. Pathogenesis of polycation-induced alterations (“fusion”) of glomerular epithelium. *Laboratory investigation; a journal of technical methods and pathology.* 1977; 36:48–61.
11. Kerjaschki D. Polycation-induced dislocation of slit diaphragms and formation of cell junctions in rat kidney glomeruli: the effects of low temperature, divalent cations, colchicine, and cytochalasin B. *Laboratory investigation; a journal of technical methods and pathology.* 1978; 39:430–440.
12. Kurihara H, Anderson JM, Kerjaschki D, et al. The altered glomerular filtration slits seen in puromycin aminonucleoside nephrosis and protamine sulfate-treated rats contain the tight junction protein ZO-1. *The American journal of pathology.* 1992; 141:805–816. [PubMed: 1415478]
13. Andrews PM. Glomerular epithelial alterations resulting from sialic acid surface coat removal. *Kidney Int.* 1979; 15:376–385. [PubMed: 513496]
14. Gelberg H, Healy L, Whiteley H, et al. In vivo enzymatic removal of alpha 2-->6-linked sialic acid from the glomerular filtration barrier results in podocyte charge alteration and glomerular injury. *Laboratory investigation; a journal of technical methods and pathology.* 1996; 74:907–920.
15. Doyonnas R, Kershaw DB, Duhme C, et al. Anuria, omphalocele, and perinatal lethality in mice lacking the CD34-related protein podocalyxin. *The Journal of experimental medicine.* 2001; 194:13–27. [PubMed: 11435469]
16. Kavoura E, Gakiopoulou H, Paraskevaku H, et al. Immunohistochemical evaluation of podocalyxin expression in glomerulopathies associated with nephrotic syndrome. *Hum Pathol.* 2011; 42:227–235. [PubMed: 21106221]
17. Copelovitch L, Guttenberg M, Pollak MR, et al. Renin-angiotensin axis blockade reduces proteinuria in presymptomatic patients with familial FSGS. *Pediatr Nephrol.* 2007; 22:1779–1784. [PubMed: 17530296]
18. Kaplan JM, Kim SH, North KN, et al. Mutations in ACTN4, encoding alpha-actinin-4, cause familial focal segmental glomerulosclerosis. *Nature genetics.* 2000; 24:251–256. [PubMed: 10700177]
19. Weins A, Kenlan P, Herbert S, et al. Mutational and Biological Analysis of alpha-actinin-4 in focal segmental glomerulosclerosis. *Journal of the American Society of Nephrology : JASN.* 2005; 16:3694–3701. [PubMed: 16251236]
20. Brown EJ, Schlondorff JS, Becker DJ, et al. Mutations in the formin gene INF2 cause focal segmental glomerulosclerosis. *Nature genetics.* 2010; 42:72–76. [PubMed: 20023659]
21. Winn MP, Conlon PJ, Lynn KL, et al. A mutation in the TRPC6 cation channel causes familial focal segmental glomerulosclerosis. *Science.* 2005; 308:1801–1804. [PubMed: 15879175]
22. Reiser J, Polu KR, Moller CC, et al. TRPC6 is a glomerular slit diaphragm-associated channel required for normal renal function. *Nature genetics.* 2005; 37:739–744. [PubMed: 15924139]
23. Michael AF, Blau E, Vernier RL. Glomerular polyanion. Alteration in aminonucleoside nephrosis *Lab Invest.* 1970; 23:649–657. [PubMed: 4098608]
24. Mohos SC, Skoza L. Glomerular sialoprotein. *Science.* 1969; 164:1519–1521. [PubMed: 5786643]
25. Wegner B, Al-Momany A, Kulak SC, et al. CLIC5A, a component of the ezrin-podocalyxin complex in glomeruli, is a determinant of podocyte integrity. *American journal of physiology Renal physiology.* 2010; 298:F1492–1503. [PubMed: 20335315]

26. Takeda T, McQuistan T, Orlando RA, et al. Loss of glomerular foot processes is associated with uncoupling of podocalyxin from the actin cytoskeleton. *J Clin Invest*. 2001; 108:289–301. [PubMed: 11457882]
27. Sun H, Schlondorff JS, Brown EJ, et al. Rho activation of mDia formins is modulated by an interaction with inverted formin 2 (INF2). *Proceedings of the National Academy of Sciences of the United States of America*. 2011; 108:2933–2938. [PubMed: 21278336]
28. Weins A, Schlondorff JS, Nakamura F, et al. Disease-associated mutant alpha-actinin-4 reveals a mechanism for regulating its F-actin-binding affinity. *Proceedings of the National Academy of Sciences of the United States of America*. 2007; 104:16080–16085. [PubMed: 17901210]
29. Pierchala BA, Munoz MR, Tsui CC. Proteomic analysis of the slit diaphragm complex: CLIC5 is a protein critical for podocyte morphology and function. *Kidney international*. 2010; 78:868–882. [PubMed: 20664558]
30. Orlando RA, Takeda T, Zak B, et al. The glomerular epithelial cell anti-adhesin podocalyxin associates with the actin cytoskeleton through interactions with ezrin. *Journal of the American Society of Nephrology : JASN*. 2001; 12:1589–1598. [PubMed: 11461930]
31. Fukasawa H, Obayashi H, Schmieder S, et al. Phosphorylation of podocalyxin (Ser415) Prevents RhoA and ezrin activation and disrupts its interaction with the actin cytoskeleton. *Am J Pathol*. 2011; 179:2254–2265. [PubMed: 21945805]
32. Takeda T, Go WY, Orlando RA, et al. Expression of podocalyxin inhibits cell-cell adhesion and modifies junctional properties in Madin-Darby canine kidney cells. *Mol Biol Cell*. 2000; 11:3219–3232. [PubMed: 10982412]
33. Yu CY, Chen JY, Lin YY, et al. A bipartite signal regulates the faithful delivery of apical domain marker podocalyxin/Gp135. *Mol Biol Cell*. 2007; 18:1710–1722. [PubMed: 17332505]
34. Fukasawa H, Obayashi H, Schmieder S, et al. Phosphorylation of podocalyxin (Ser415) Prevents RhoA and ezrin activation and disrupts its interaction with the actin cytoskeleton. *The American journal of pathology*. 2011; 179:2254–2265. [PubMed: 21945805]
35. Schmieder S, Nagai M, Orlando RA, et al. Podocalyxin activates RhoA and induces actin reorganization through NHERF1 and Ezrin in MDCK cells. *Journal of the American Society of Nephrology : JASN*. 2004; 15:2289–2298. [PubMed: 15339978]
36. Meder D, Shevchenko A, Simons K, et al. Gp135/podocalyxin and NHERF-2 participate in the formation of a preapical domain during polarization of MDCK cells. *The Journal of cell biology*. 2005; 168:303–313. [PubMed: 15642748]
37. Li H, Durbin R. Fast and accurate short read alignment with Burrows-Wheeler transform. *Bioinformatics*. 2009; 25:1754–1760. [PubMed: 19451168]
38. McKenna A, Hanna M, Banks E, et al. The Genome Analysis Toolkit: a MapReduce framework for analyzing next-generation DNA sequencing data. *Genome research*. 2010; 20:1297–1303. [PubMed: 20644199]
39. DePristo MA, Banks E, Poplin R, et al. A framework for variation discovery and genotyping using next-generation DNA sequencing data. *Nature genetics*. 2011; 43:491–498. [PubMed: 21478889]

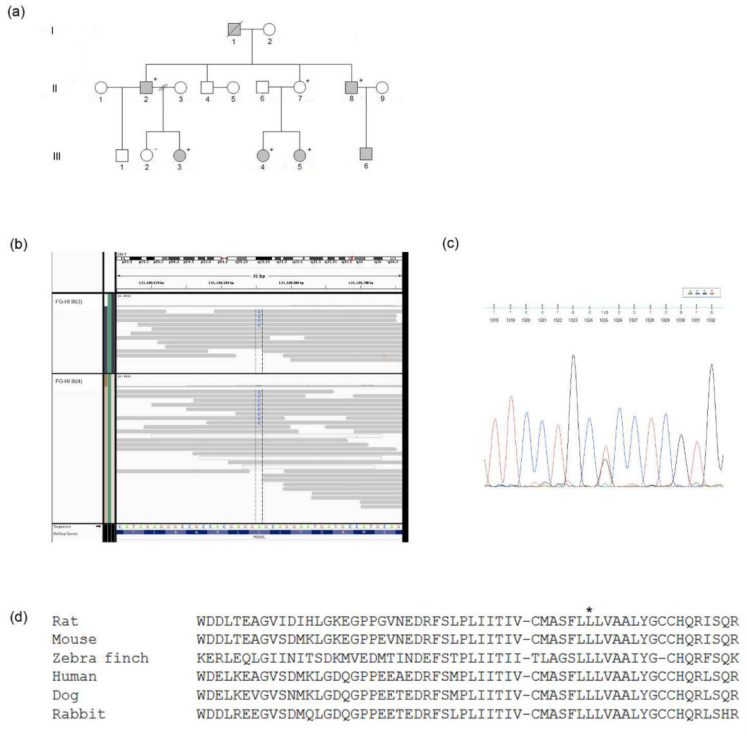


Figure 1. Pedigree of family FG-HI, sequencing and multisequence alignment. (a) Pedigree for family FG-HI. Affected individuals are indicated in grey. Individuals who are heterozygous for the variant PODXL p.L442R are denoted by “+” while those without the mutation are denoted by “-”. Individuals without a notation were not tested because no sample was available. (b) Next-generation sequencing reads across PODXL aligned to the reference genome in Integrative Genome Viewer (IGV). The antisense strand is indicated as reference. (c) Sanger sequencing confirming the PODXL variant in all affected individuals where DNA was available. The sense strand is indicated. (d) Multisequence alignment showing conservation of the affected amino acid residue, p.442L indicated with an “*”.

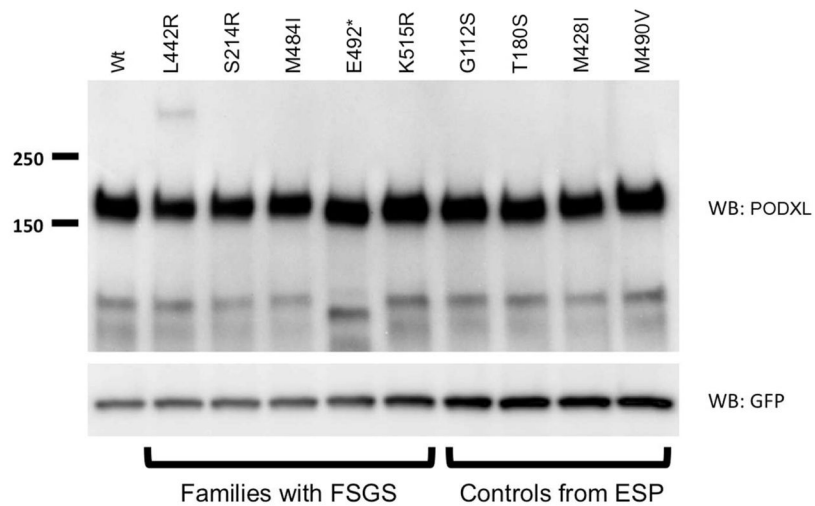


Figure 2.

FSGS-associated genetic variants do not alter the stability of PODXL protein. MDCK cells were co-transfected with GFP and equal amounts of either wildtype PODXL plasmid, PODXL plasmid containing an FSGS-associated variant (p.L442R to p.K515R), or PODXL plasmid containing a control variant from the Exome Sequencing project (p.G112S to p.M490V). After 24 h, the cells were lysed, and the lysates were immunoblotted for PODXL (upper panel) or GFP (lower panel). * indicates amino acid is deleted.

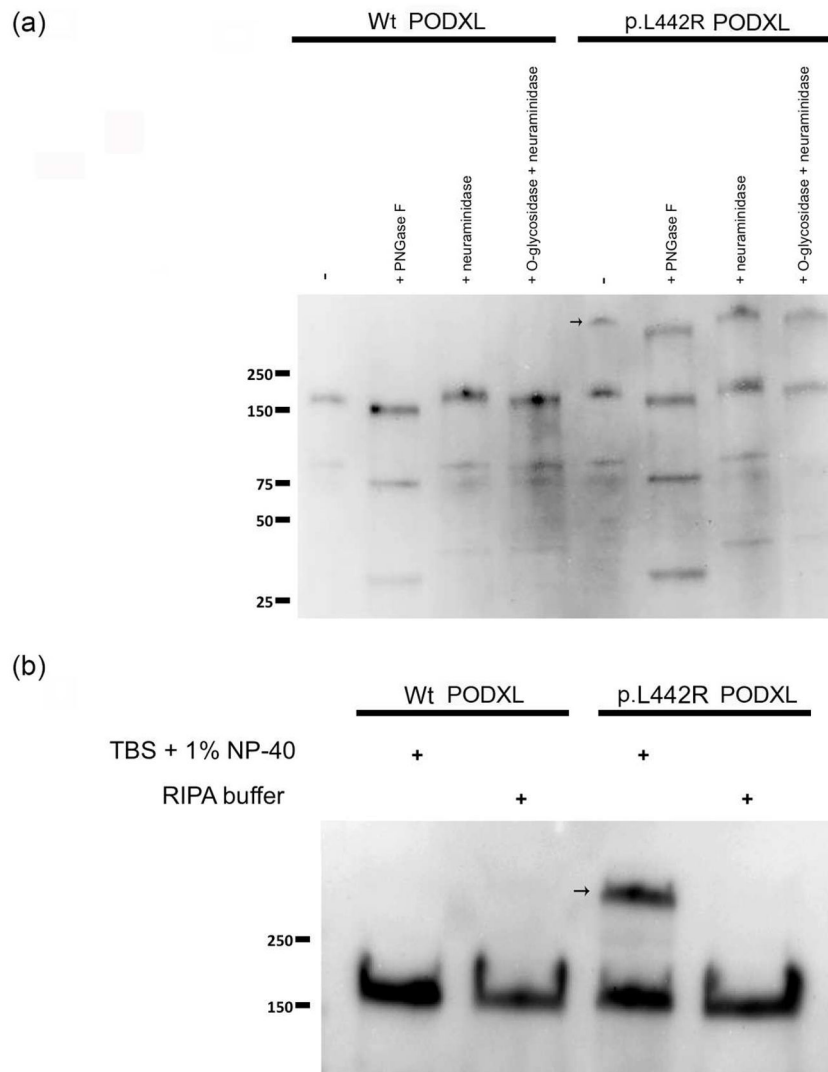


Figure 3.

The FSGS-associated p.L442R variant induces the formation of PODXL dimers. (a) MDCK cells transfected with either wildtype or p.L442R PODXL plasmid were mock treated or treated with either PNGase F, neuraminidase, or a combination of O-glycosidase and neuraminidase. No differences were observed before or after deglycosylation patterns in both PODXL wildtype and p.L442R mutant on Western blotting. (b) MDCK cells were transfected with either PODXL wildtype plasmid or PODXL p.L442R plasmid. The cells were lysed after 24 h in either mild lysis buffer (TBS + 1% NP-40) or lysis buffer with ionic detergent (RIPA). PODXL was detected using an anti-PODXL antibody. Arrows indicates upper form.

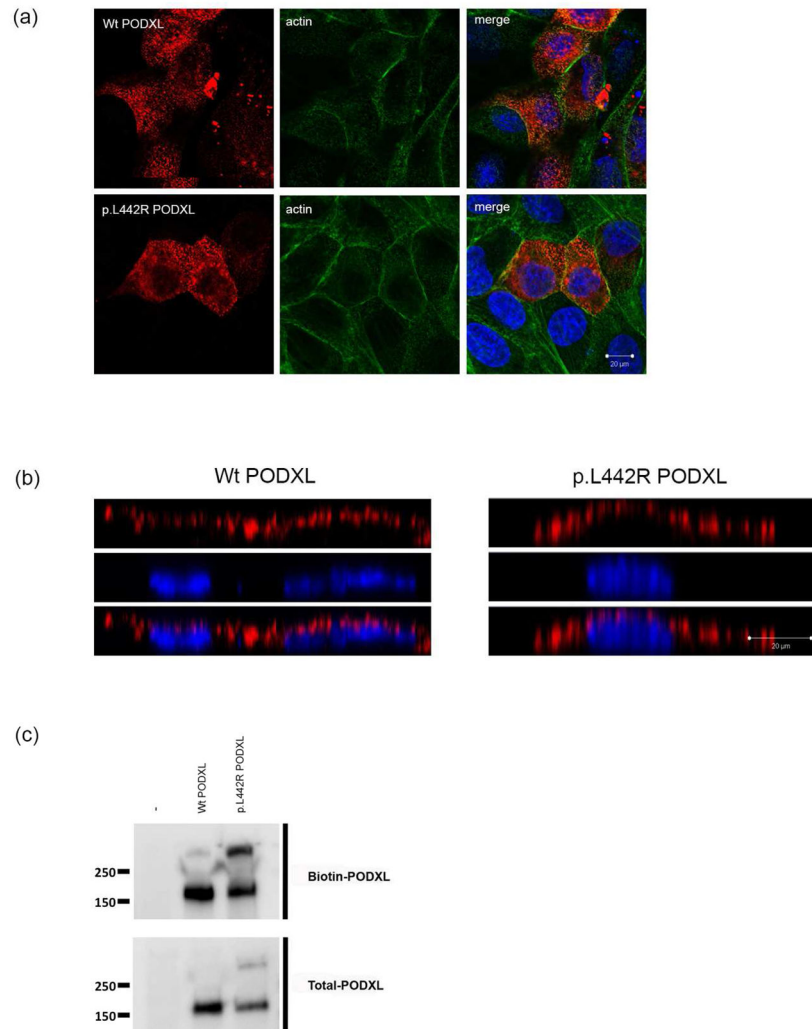


Figure 4. The FSGS-associated p.L442R variant does not alter the subcellular localization of PODXL. MDCK cells transfected with PODXL wildtype or p.L442R plasmid. PODXL was labeled with an anti-PODXL antibody (red), F-actin was labeled with phalloidin (green), and nuclei were labeled with Hoechst 33342 (blue). (a) Horizontal slices of confocal stacks. (b) Vertical slices of confocal stacks. (c) Transfected MDCK cells were surface biotinylated, and cell surface proteins were pulled down using streptavidin beads. Total PODXL and biotinylated PODXL were visualized by Western blot.

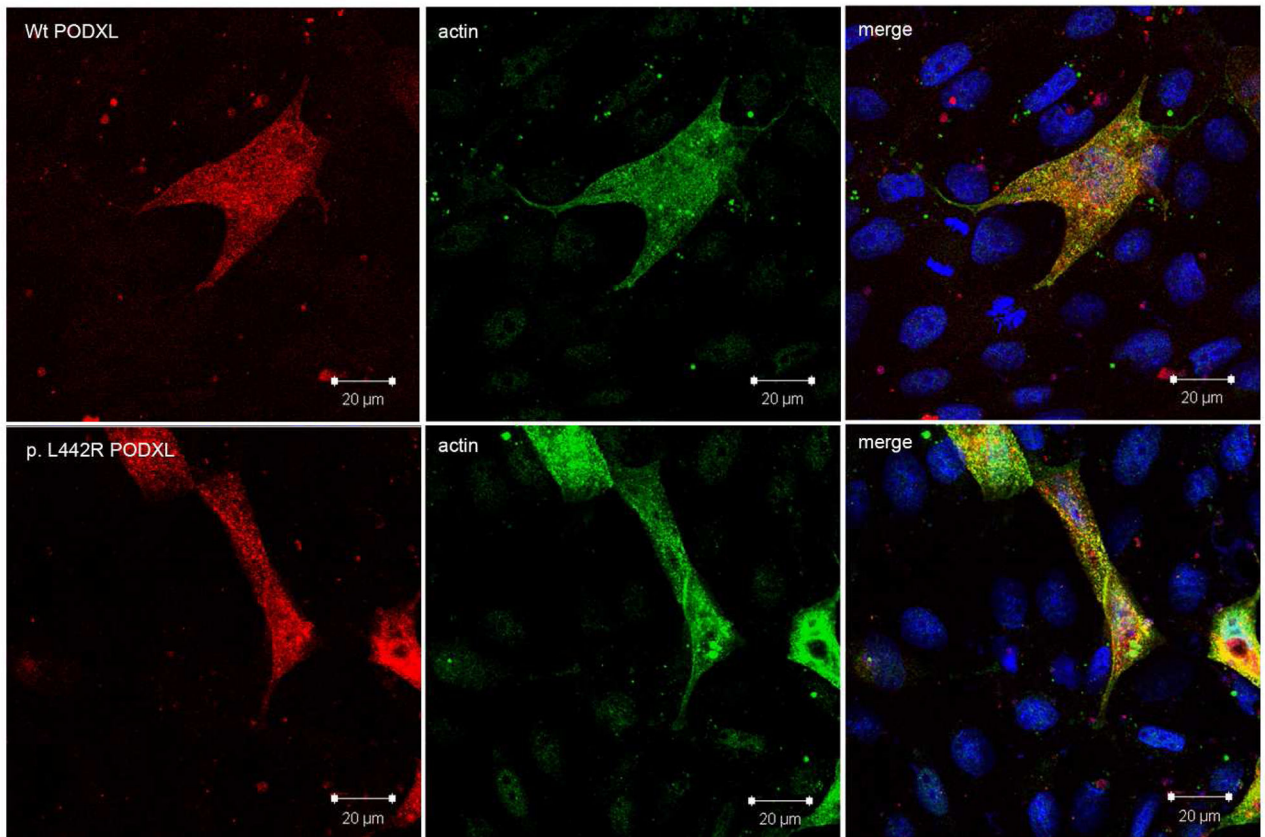


Figure 5.

The FSGS-associated L442R variant does not alter co-localization of PODXL with ezrin at the apical surface. MDCK cells co-transfected with ezrin and either wildtype or p.L442R PODXL plasmid were fixed. PODXL was labeled with an anti-PODXL antibody (red) and GFP-tagged ezrin was labeled with anti-GFP antibody (green). Scale bar: 20 µm.

PODXL rare variants discovered in the FSGS cohort and selected *PODXL* rare variants from the Exome Sequencing Project (ESP). The number of alleles with the indicated variant found in the 1000 Genomes Project (1KG) and ESP are indicated in columns 7 and 8. At the time of reference, sequence information for 2200 and 10800 haplotypes was available in the 1KG and ESP, respectively. All of these variants were introduced by mutagenesis in plasmids harboring the *PODXL* gene for further experiments. Amino acid changes are indicated using NCBI accession number NM_005397. DNA coordinates are indicated in reference to human Hg19.

Table 1

Cohort	CODON CHANGE	AMINO ACID CHANGE	MUTATION TYPE	LOCATION	POSITION	1KG	ESP
FSGS	agC/agA	p.S214R	Missense	Extracellular	131195651	0	0
FSGS	cTc/cGc	p.L442R	Missense	TM	131190685	0	0
FSGS	atG/atA	p.M484I	Missense	Intracellular	131189199	0	3
FSGS	* GAG/-	p.E492-	Deletion	Intracellular	131189174	61	NA
FSGS	aAg/aGg	p.K515R	Missense	Intracellular	131189107	0	6
ESP	Ggc/Agc	p.G112S	Missense	Extracellular	131195959	-	3773
ESP	Acc/Tcc	p.T180S	Missense	Extracellular	131195755	-	4
ESP	atG/atA	p.M428I	Missense	TM	131190726	-	1
ESP	Atg/Gtg	p.M490V	Missense	Intracellular	131189183	-	1

* indicates in-frame deletion, TM = transmembrane